



The Microstructure of Continuously Cooled Tough Bainitic Steels

¹ F.G. Caballero, ¹ C. Capdevila, ¹ J. Chao, ¹ J. Cornide and ¹ C. Garcia-Mateo,
² H. Roelofs, ² St. Hasler and ² G. Mastrogiacomo

¹ Spanish National Center for Metallurgical Research (CENIM-CSIC), SPAIN

² Swiss Steel AG, Emmenweidstraße 90, 6021 Emmenbrücke, SWITZERLAND

2nd Int Conf. Super-High Strength Steels

THE MICROSTRUCTURE OF CONTINUOUSLY COOLED TOUGH BAINITIC STEELS

F.G. Caballero, C. Capdevila, J. Chao, J. Cornide and C. Garcia-Mateo – Spanish National Center for Metallurgical Research (CENIM-CSIC), Spain
H. Roelofs, St. Hasler and G. Mastrogiacomo – Swiss Steel AG, Switzerland

ABSTRACT

The influence of bainite morphology on the impact toughness behaviour of a continuously cooled cementite free low carbon C-Mn-B type of steel has been examined. Different bainite morphologies were obtained by cooling from the austenite regime to ambient temperature with different cooling rates. The resulting microstructures have been quantitatively analysed using light optical microscopy (LOM), scanning electron microscopy (SEM) and electron back scatter diffraction (EBSD) techniques. The relationship between the steel morphology and impact toughness has been discussed. It could be shown that bainitic microstructures formed mainly by lath-like upper bainite, consisting of thin and long parallel ferrite laths, exhibit higher impact toughness values than those with a granular bainite morphology, consisting of an equiaxed ferrite structure and discrete islands of M/A phases. Granular bainite shows evidence of low resistance to crack propagation during cleavage fracture because of its larger crystallographic packet size. Moreover, the stress concentration associated with coarse M/A grains is considered as a possible factor contributing to the premature crack nucleation.

KEYWORDS

Impact toughness, cementite-free bainite, bainite morphology, electron back scatter diffraction (EBSD), low carbon steel

INTRODUCTION

It is clear that the term bainite describes a variety of different complex microstructures that offer diverse combinations of strength and toughness. The well-known difference in carbide distribution between bainite formed at high and low temperatures, viz., intralath and interlath, respectively, appears to exist in a majority of steels and makes the classical nomenclature of upper and lower bainite useful, both in describing the microstructural appearance and in classifying the overall reaction mechanism. In upper bainite, the carbides precipitate from carbon-enriched residual austenite. Upper bainitic ferrite itself is free from precipitates. The precise role of intra-ferrite carbides in lower bainite formation is not clear. There are many observations that reveal that lower bainitic cementite nucleates and grows within supersaturated ferrite in a process identical to the tempering of martensite [1]. The slower diffusion associated with the reduced transformation temperature provides an opportunity for some of the carbon to precipitate in the supersaturated bainitic ferrite. A fine dispersion of plate-like carbides is then found inside the ferrite plates, with a single crystallographic variant within a given ferrite plate, although it is possible to observe more than one variant of carbide precipitation in a lower bainite sub-unit [1,2].

In literature other categorization schemes for the description of bainite have been proposed [3-6]. More recently, S. Zajac et al. [7] provide a unified terminology, which may be applied for both low-carbon and high-carbon bainite. In this new classification, bainite is divided into three main groups depending on ferrite morphology and the type and distribution of second phases: i) Granular bainite with irregular ferrite; ii) Upper bainite with lath-like ferrite and the second phases on lath

boundaries; and iii) Lower bainite, lath-like or plate-like, with cementite within the ferrite plates or laths. The microstructure of low carbon high strength steels, composed of bainitic ferrite with M/A constituents is called carbide free bainite in the Ohmori et al. classification [4,5]. This bainite is, however, similar to the granular bainite at the micro-scale. The upper bainite which does not contain carbides but the M/A constituents is called degenerated upper bainite by Zajac et al. [7]. Lower bainite having cementite forming within the ferrite crystal is divided into two groups which have either lath morphology, typical for low-carbon steels or plate morphology which is typical for lower bainite in steels with higher carbon levels.

Depending on the cooling curve precipitation of cementite during bainitic transformation might be suppressed in low carbon steels [4]. The resulting microstructure than consists of bainitic ferrite and M/A constituent. In this paper we will refer to this microstructure as cementite free bainite. The formation of lower bainite is not inhibited in these steels. Therefore, only granular bainite and degenerated upper bainite morphologies, following Zajac et al. classification, can be considered as a cementite free bainitic microstructure in these steels. In this paper we will refer to these morphologies as granular bainite and cementite free lath-like upper bainite as Fig. 1 shows.


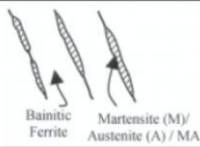
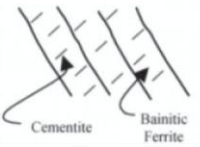
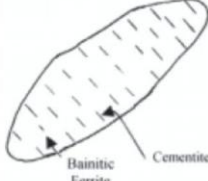
| Bainite | Morphology | Bainite description |
|---|---|---|
| Granular bainite | Irregular ferrite with M/A. |  Martensite/MA Bainitic Ferrite |
| Cementite-free lath-like upper bainite | Lath-like ferrite with M/A on lath boundaries. |  Bainitic Ferrite Martensite (M)/Austenite (A) / MA |
| Lath-like lower bainite | Lath-like ferrite with cementite inside the ferrite laths |  Cementite Bainitic Ferrite |
| Plate-like lower bainite | Plate-like ferrite with cementite inside the ferrite plates |  Bainitic Ferrite Cementite |

Fig. 1. Morphological classification used in this work for cementite free bainitic steels.

In the present work a commercial hot rolled low carbon C-Mn-B steel [8,9] was used to adjust different steel microstructures by varying the cooling conditions. The resulting cementite-free bainitic microstructures have been quantitatively analysed using light optical microscopy (LOM), scanning electron microscopy (SEM) and electron back scatter diffraction (EBSD) techniques and the relationship between the morphology and impact toughness of bainite has been discussed.

1. EXPERIMENTAL PROCEDURE

A commercial microalloyed C-Mn-B type of steel with a tensile strength level of ~800 MPa was chosen for this study. The steel was conventionally hot rolled to a 15 mm wire rod. The cooling rate between 800°C and 500°C was estimated to be 1.5 °C/s.

To simulate the influence of different cooling rates 10x10x80 mm samples were re-austenized at 910°C in a Gleeble machine and cooled to room temperature with 3.0, 5.0, 7.0, 9.0 and 11.0 °C/s, respectively.

Table 1.- Chemical composition of the studied steel, (wt-%).

| C | Si | Mn | Ni | Cr | Mo | V | Ti | B | N |
|------|------|------|------|------|-------|------|------|--------|--------|
| 0.07 | 0.21 | 1.86 | 0.10 | 0.11 | 0.024 | 0.04 | 0.08 | 15 ppm | 99 ppm |

Impact energies were measured on Charpy V-notched (10x10 mm²) samples at room temperature using a 300 J Charpy testing machine. Specimens were tested in accordance with standard DIN EN 10045-1: 1990. The impact strength values in J/ cm² were used for comparison. Three samples with low (1.5 °C/s), intermediate (3.0 °C/s) and high (9.0 °C/s) impact strength were chosen for detailed analysis of their microstructure.

A 2 pct Nital etching solution was used to reveal the microstructure by LOM. To investigate more in detail the microstructure of the steel, SEM was carried out on a Jeol JSM-6500F field emission scanning electron microscope operating at 7 kV. The volume fraction and size of M/A constituent were deduced from standard quantitative metallographic method on SEM micrographs at a magnification of x1500-x2000.

Quantitative X-ray analysis was used to determine the fraction of retained austenite. After grinding and final polishing using 1 µm diamond paste, the samples were etched to obtain an undeformed surface. They were then step-scanned in a SIEMENS D 5000 X-ray diffractometer operating at 40 kV and 30 mA and using unfiltered Cu K_α radiation. The EBSD scans were carried out in a Jeol JSM-6500F equipped with a TSL MSC 2200 EBSD system in the same samples.

2. RESULTS AND DISCUSSION

By raising the cooling rate from 1.5 to 9.0 °C/s the Charpy impact strength of the considered steel is continuously improved (Table 2). But at the next higher cooling rate of 11.0 °C/s the impact strength is lower again. A larger martensite contribution accompanied by larger martensite islands is supposed to be the reason for this. To study the influence of the bainite substructure on the Charpy impact strength three samples with low (1.5 °C/s), intermediate (3.0 °C/s) and high (9.0 °C/s) impact strength were selected for deeper analysis.

Table 2.- Hardness and impact strength

| Cooling rate | HV30 | ISO-V (J/cm ²) | Remarks |
|--------------|----------|----------------------------|--|
| 11.0 °C/s | 282 ± 6 | 118 J/cm ² | Re-austenized at 910°C in a Gleeble machine |
| 9.0 °C/s | 285 ± 9 | 208 J/cm ² | Re-austenized at 910°C in a Gleeble machine, V-notched sample used for structural analysis |
| 7.0 °C/s | 276 ± 12 | 165 J/cm ² | Re-austenized at 910°C in a Gleeble machine |
| 5.0 °C/s | 253 ± 18 | 118 J/cm ² | Re-austenized at 910°C in a Gleeble machine |
| 3.0 °C/s | 254 ± 10 | 121 J/cm ² | Re-austenized at 910°C in a Gleeble machine, V-notched sample used for structural analysis |
| 1.5 °C/s | 257 ± 9 | 39 J/cm ² | As hot rolled, V-notched sample used for structural analysis |

Fig. 2 illustrates LOM and SEM micrographs of these samples. Austenitic grain sizes were expected to be $\sim 30\mu\text{m}$. The contributions of bainite, martensite and retained austenite were quantitatively analyzed. No evidence of allotriomorphic ferrite was found. The results are presented in Table 3. These data and the micrographs reveal that all the samples have a microstructure consisting of mainly cementite free bainitic ferrite and M/A constituent. Two different morphologies of bainite have been identified depending on the cooling rate: lath-like upper bainite, consisting of thin and long parallel ferrite laths, and granular bainite, consisting of an equiaxed ferrite structure with discrete islands of M/A phases.

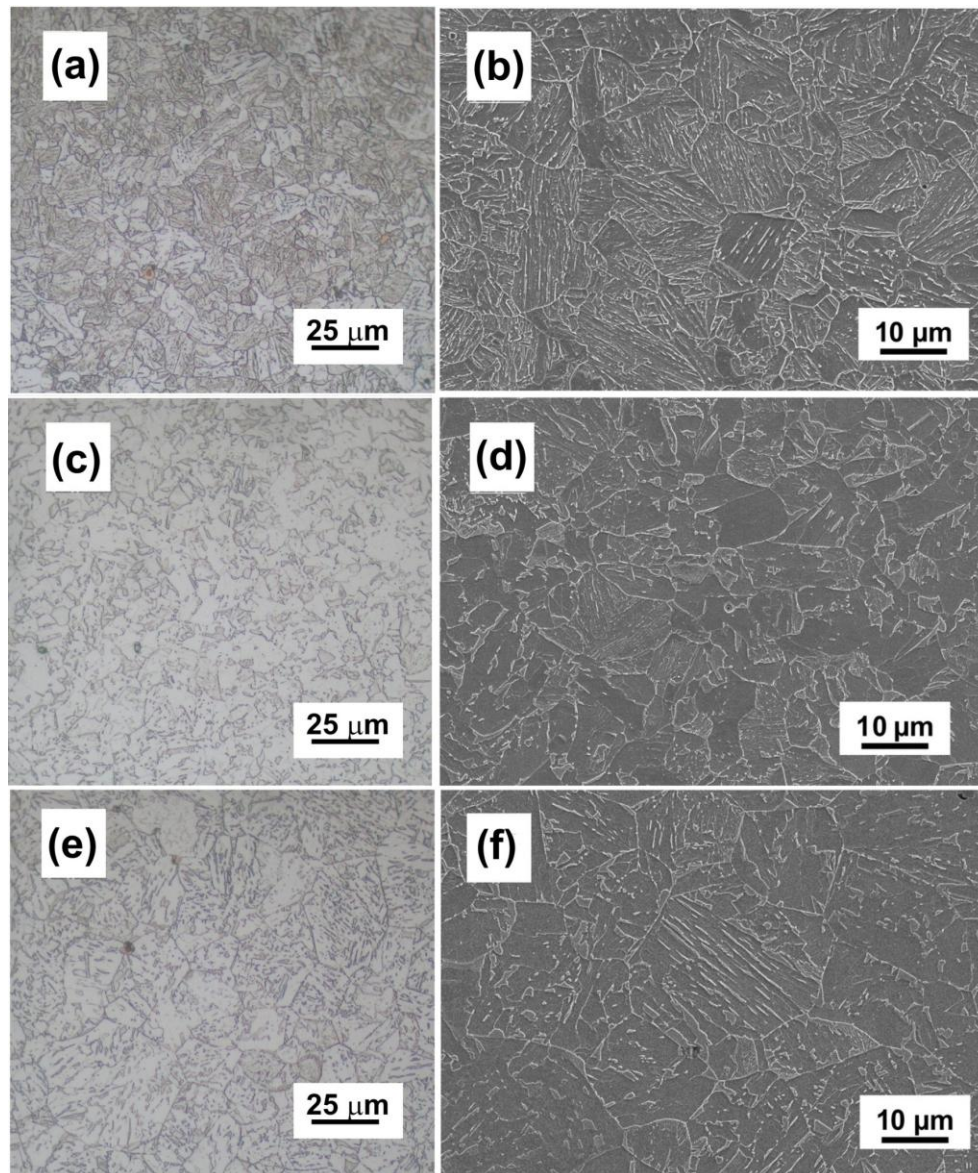


Fig. 2. Light optical and scanning electron micrographs of a low carbon bainitic steel after continuously cooling at: (a) and (b) $9\text{ }^{\circ}\text{C/s}$; (c) and (d) $3\text{ }^{\circ}\text{C/s}$; and (e) and (f) $1.5\text{ }^{\circ}\text{C/s}$.

Table 3.- Quantitative analysis of microstructure

| Cooling Rate | V_B | V_M | V_γ |
|--------------|-------------|-------------|-------------|
| 9 °C/s | 0.87 ± 0.04 | 0.12 ± 0.03 | 0.01 ± 0.01 |
| 3 °C/s | 0.93 ± 0.04 | 0.05 ± 0.03 | 0.02 ± 0.01 |
| 1.5 °C/s | 0.90 ± 0.03 | 0.08 ± 0.02 | 0.02 ± 0.01 |

V_B is the volume fraction of bainitic ferrite; V_M is the volume fraction of martensite; V_γ is the volume fraction of retained austenite; and x_γ is the carbon content in austenite.

Further differences in the bainite morphology can be deduced from the SEM micrographs as shown in Figs. 2. The sample cooled at 9 °C/s shows thin, long and slender well defined laths (see Fig. 2.b), meanwhile the nature of bainite in the samples cooled at 3 °C/s and 1.5 °C/s seems to be coarser (see Fig. 2.d and 2.f). Moreover, the microstructure in the samples cooled at 3 and 1.5 °C/s exhibits a distribution of equiaxed M/A grains within the bainitic ferrite matrix, instead of very thin films between subunits within a given sheaf of bainite. It is also observed that the lower cooling rate leads to coarser M/A grains inside the granular bainite. Table 4 summarises the results of the quantitative structure analysis.

Table 4.- Quantitative data on the M/A grain size distribution

| Cooling Rate | Morphology of Bainite | M/A Grain Size, μm (Shape of M/A) | Maximum M/A Grain Size, μm |
|--------------|-----------------------|---|---------------------------------------|
| 9 °C/s | Mainly LLUB. | 0.12±0.03 (Thin Films in LLUB) | 0.18 |
| 3 °C/s | Mainly GB | 1.30±0.89 (Equiaxed Grains in GB) | 3.61 |
| 1.5 °C/s | Mainly GB | 1.73±0.84 (Equiaxed Grains in GB) | 5.61 |

LLUB is lath-like upper bainite; GB is granular bainite.

Impact toughness values achieved in bainitic microstructures are generally attributed to the amount of martensite, V_M . In principle, the presence of a very hard phase, such as martensite, in a bainitic microstructure, would deteriorate toughness as it has been extensively reported [10-12]. However, Chatterjee and Bhadeshia [13] proposed and showed experimentally that the load transfer into the hard martensite becomes similarly difficult as the scale of the martensite decreases in a relatively soft matrix. In other words, the martensite will not crack easily if its size is reduced below some critical value typically around 10 μm . Naturally, work hardening comes into this scenario so that sufficient load should eventually be transferred into the martensite to cause fracture. However, the stage at which this occurs ought to be delayed when the martensite is fine.

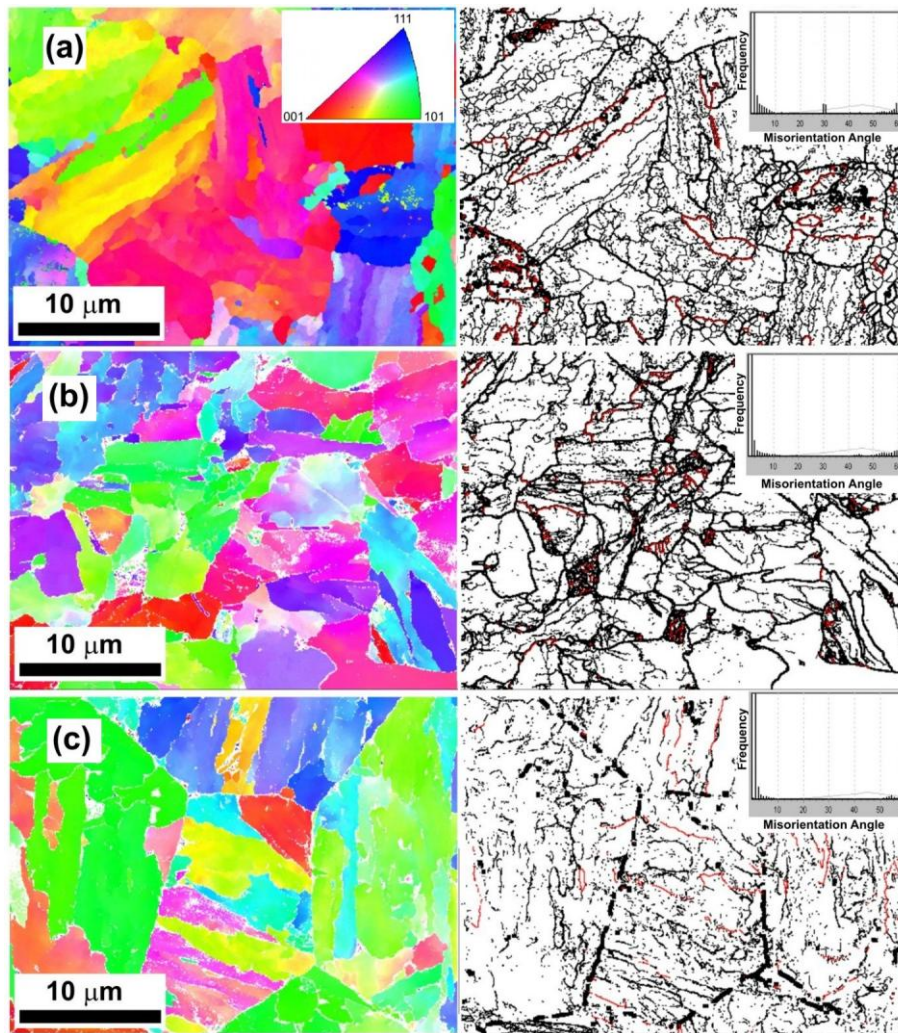


Fig. 3. Orientation imaging map, misorientation map (tolerance angle of 15°) and corresponding misorientation frequency graph of (a) lath-like upper bainite in sample cooled at 9°C/s and granular bainite in samples cooled at: (b) 3°C/s and (c) 1.5°C/s .

Results in Table 2 and 3 suggest that the amount of martensite in the microstructure does not explain the toughness behaviour of the investigated samples. The sample with a martensite volume fraction of 0.05 ± 0.03 in the bainitic microstructure reaches a lower impact strength value (121 J/cm^2) than the sample with a martensite volume fraction of 0.12 ± 0.03 (208 J/cm^2). The size distribution of the M/A phase (films and grains) was also quantitative determined in the studied samples. Table 4 lists mean values of the size of the M/A films present in lath-like upper bainite and equiaxed M/A grains in granular bainite. The films of M/A constituents present in lath like upper bainite are remarkable small ($\sim 0.13 \mu\text{m}$) in comparison to the M/A grains in granular bainite ($\sim 1.5 \mu\text{m}$). In case of a granular bainitic microstructure differences in M/A grain size might affect impact toughness. There is some indication that the presence of coarse equiaxed martensite islands with a diameter of $4\text{-}6 \mu\text{m}$ might cause brittle behaviour in these bainitic microstructures.

In addition to the coarse M/A grains, fracture may be controlled by microstructural features such as bainite packets [14-17]. Bainite is a microstructure made up of packets of parallel plates in the so-called morphological packet. The good toughness of this microstructure is related to the high density of the high-angle boundaries that these microstructures usually present [18]. This kind of boundaries acts as obstacles to cleavage propagation, forcing the cleavage crack to change the

microscopic plane of propagation in order to accommodate the new local crystallography [19]. Low-angle boundaries are not effective obstacles and, consequently, seem to have no influence on the toughness of steels. For this reason, from the point of view of the fracture mechanics, it is convenient to use the concept of a effective crystallographic packet [18], defined as the continuous set of ferrite plates with a crystallographic misorientation lower than a certain angle (here 15°).

Figure 3 illustrates the differences on the type of grain boundaries (low or high angles) and grain boundaries misorientation between lath-like upper bainite (Fig. 3.a) and granular bainite (Fig. 3.b and 3.c). It is clear from the misorientation map that the effective crystallographic packet in lath-like upper bainite is finer than in granular bainite.

Therefore, differences in the type of grain boundaries (low or high angles) and grain boundaries misorientation will also explain the difference toughness response of both morphologies of bainite [20]. Granular bainite is an equiaxed structure, containing discrete island of M/A phases, and has low toughness by forming relatively large effective crystallographic packets. By contrast, lath-like upper bainite exhibits a good combination of strength and toughness since it has high interior dislocation density and fine effective grains.

The SEM micrographs of the cleavage fracture surface of impact specimens tested at room temperature are shown in Fig. 4. Although it was possible to identify fracture initiation site by tracing river lines to an origin on low magnification micrographs, the initiation site itself was usually featureless. The identification of the cracks and/or voids nucleation sites in these microstructures is currently under investigation, but it is believed that hard M/A grains are most susceptible for microvoids and/or microcracks nucleation [12,21].



Fig. 4. Cleavage fracture surface of impact specimens tested at room temperature in a low carbon bainitic steel after continuous cooling at: (a) 9 °C/s; (b) 3 °C/s; and (c) 1.5 °C/s. The arrow identifies a fracture initiation site.

Fractographs in Fig. 4 suggest that the samples cooled at 3 and 1.5 °C/s with granular bainite morphology exhibit coarser transgranular facets in the cleavage fracture surface than those for the sample cooled at 9 °C/s with a lath-like upper bainite morphology. This increase on the facet size detected on microstructures with granular bainite morphology must be closely related to the increase on the bainite packet size observed by EBSD analysis. Morris et al [22] clearly illustrated that relationship in as-quenched a 9Ni steel using profile SEM fractographs of cleavage fracture. The steel is cleaved along {100} planes that cross many laths within packet, meanwhile the crack branches at packet boundaries where the orientation of the {100} planes changes.

Therefore, the brittle fracture of continuously cooled cementite-free bainitic steels is governed by the extension of fast microcracks across bainitic ferrite boundaries. Hard brittle phases such as M/A grains have an essential, intermediate role because, unlike the ferrite, they permit the crack nucleus to form without blunting it. The brittle fracture stress will then depend of two quantities: i) the size of the microcrack which corresponds with the M/A grain dimensions; and ii) the resistance that the microcrack experiences when it attempts to cross the boundary. The microstructural feature whose boundaries resist microcrack extension in the studied steels has been found to be the bainite packets.

3. CONCLUSIONS

Microstructural characterisation and impact toughness evaluation of different continuously cooled cementite-free bainitic microstructures have demonstrated that bainitic microstructures formed mainly by lath-like upper bainite, consisting of thin and long parallel ferrite laths, exhibits higher impact toughness values than those with a granular bainite morphology, consisting of an equiaxed ferrite structure and discrete islands of M/A phases. Results suggest that the mechanism of brittle fracture of cementite free bainitic steels involves nucleation of microvoids and/or microcracks in M/A grains but is controlled by the bainite packet size.

ACKNOWLEDGMENTS

J. Cornide acknowledges the Spanish Ministry of Science and Innovation for financial support in the form of a PhD research grant (FPI).

REFERENCES

1. H.K.D.H. BHADSHIA, *Acta Metall.* 28, (1980), p.1103.
2. L.C. CHANG, *Mater. Sci. Eng. A* 368A, (2004), p.175.
3. Y. OHMORI, H. OHTANI and T. KUNITAKE, *Trans. Iron Steel Inst. Jpn.* 11, (1971), p. 250.
4. H. OHTANI, S. OKAGUCHI, Y. FUJISHIRO and Y. OHMORI, *Metall. Trans. A* 21A, (1990), p. 877.
5. B.L. BRAMFITT and J.G. SPEER, *Metall. Trans. A* 21A, (1990), p.817.
6. G. KRAUSS and S.W. THOMSON, *ISIJ Inter.* 35, (1995), p.937.
7. S. ZAJAC, J. KOMENDA, P. MORRIS, P. DIERICKX, S. MATERA and F. PENALBA DIAZ, *Technical Steel Research*, Report EUR 21245EN, Luxembourg (2005), p.10.
8. S. WAENGLER, *Freiberger Forschungshefte B344*, (2008)
9. R. KUZIAK, S. ZAJAC, R. KAWALLA, S. WAENGLER, K. STERCKEN, J. NOACK, M. SAFI, R. JAKUBCZAK, R. URLAU, S. HASLER, L. CHABBI, *Technical Steel Research*, Report EUR 24191, Luxembourg, (2010).
10. H.K.D.H. BHADSHIA and D.V. EDMONDS, *Met. Sci.* 17, (1983), p.411.
11. H.K.D.H. BHADSHIA and D.V. EDMONDS, *Met. Sci.* 17, (1983), p.420.
12. F.G. CABALLERO, J. CHAO, J. CORNIDE, C. GARCÍA-MATEO, M.J. SANTOFIMIA and C. CAPDEVILA, *Mater. Sci. Eng. A* 525A, (2009), p.87.
13. S. CHATTERJEE and H.K.D.H. BHADSHIA, *Mater. Sci. Technol.* 22, (2006), p.645.
14. P. BROZZO, G. BUZZICHELLI, A. MASCANZONI and M. MIRABILE, *Met. Sci.* 11, (1977), p.123.
15. A. KAMADA, N. KOSHIZUKA and T. FUNAKOSHI, *Trans. Iron and Steel Inst. of Japan* 16, (1976), p.407.
16. H. KOTILAINEN, *Fracture and Fatigue*. J.C. RADON, ed., Pergamon Press, Oxford (1980), p.217.
17. H. KOTILAINEN, K. TORRONEN and P. NEONEN, *Advances in Fracture Research*. Vol. 2. D. FRANCOIS, ed., Pergamon Press, Oxford, (1982), p.723.
18. A.F. GOURGUES, H.M. FLOWER and T.C. LINDLEY, *Mater. Sci. Technol.* 16, (2000), p.26.
19. J.M. RODRÍGUEZ-IBABE, *Mater. Sci. Forum* 284–286, (1998), p.51.
20. Y.M. KIM, S.Y. SHIN, H. LEE, B. HWANG, S. LEE and N.J. KIM, *Metall. Mater. Trans. A* 38^a, (2007), p.1731.

21. D. DAS and P.P. CHATTOPADHYAY, J. Mater. Sci. 44 (2009), p.2957.
22. J.W. MORRIS, C.S. LEE and Z. GUO, ISIJ Int. 43, (2003), p.410.